Analysis of NACA 2412 Airfoil For Use As A Rear Wing On A Go Kart

To: Dr. Jacqueline L Huynh
From: Nicholas Slayton

Date of Experiment: November 23, 2021
Date: December 8, 2021

Subject: Exploration of NACA 2412 and variants for use as rear wings
Cc: Dipan Deb

Table of Contents

Nomenclature List

$a = acceleration$
$c = chord$
$C_D = Coefficient\ of\ Drag$
$C_L = Coefficient\ of\ Lift$
$D = Drag$
$F = Force$
$L = Lift$
$m = Mass$
$P = Pressure$
$r = radius$
$S = Area$
$t = Thickness$
$v = speed$

$\alpha = Angle\ of\ Attack$
$\mu = Coefficient\ of\ Friction$
$\rho = Density$

List of Figures

List of Tables

Abstract

In this report the effects of adding a rear wing to a high speed go kart are explored. The addition of rear wings to cars can prove to be advantageous for their performance. As such studying rear wing variations can prove to be highly insightful in the world of motorsport. The rear wing, in particular, that will be studied, will be modeled off of the NACA 2412 airfoil and its sizing will be based off of similar rear wings that are often attached to the chosen go kart. Unfortunately, due to sizing constraints as a result of UCI's wind tunnel small test section, a scaled model of the rear wing needed to be constructed. This was done by ensuring that the Reynolds number and Aspect ratio of the model matched those of the actual rear wing. In order to test the full potential of the NACA 2412 airfoil three variations were used. These variations being a normal, symmetrical, and reverse airfoil. The ultimate goal being that these airfoil variants could be compared, with the best variant and angle of attack being chosen to maximize the performance of the go kart. Ultimately the results outlined below in this report were more similar than expected but unfortunately performance improvements were not found.

Introduction

In the sport of motor racing the ability to maintain control at a high speed is of the utmost importance. As such over the years engineers have devised ways that not only improve stability and control at high speeds but also performance. One of these methods is through the use of a rear wing. A rear wing is a fairly simple device. In essence, it is a wing, much like one that may be found on an airplane, that has been flipped upside down so that instead of providing a lifting force the wing provides a downward force. This force, referred to as down force, allows a car to make turns at higher speeds as well as increase the amount of power that can be transferred from the car to the ground allowing for better acceleration. The mechanics of this effect are fairly simple and can be seen in the following equation

$$F_f = \mu N \quad (Equation\ 1)$$

Here the N is the normal force that the car exerts on the road, μ is the coefficient of friction, and F is the maximum force that the car can exert on the road before the tires begin to slip. As seen by the equation an increase in the normal force allows for the car to increase the force it exerts on the road. The result being that the car can accelerate faster, thus improving the performance of the car. Below is the equation that can be used to calculate this acceleration.

$$a = F/m \quad (Equation\ 2)$$

Here it is seen that as the force exerted by the car on the road increases the acceleration that can be achieved by the car increases. As such once the force is known this performance parameter for the car can be determined. In order to find the force the cars weight along with any other forces, such as downforce need to be summed together. While finding the weight of the car is trivial, finding the downforce that will be exerted by the airfoil is a slightly more complicated process.

This will be the main focus of the experiment that is presented in this report. By placing an accurately scaled model of the desired rear wing into a wind tunnel, force measurements taken at different angles of attack can be used to calculate the different coefficient of lift as a function of an angle of attack. The equations for doing so are as follows.

$$L = Ncos(\alpha) - Asin(\alpha) \quad (Equation\ 3)$$

$$L = \frac{1}{2} C_L \rho v^2 S \quad (Equation\ 4)$$

$$C_L = \frac{L}{\frac{1}{2}\rho v^2 S} \quad (Equation\ 5)$$

As shown by the equations above, once the coefficient of lift is found the expected lift force that will be generated by the airfoil can be found. Of course in this report's case the lift force is actually the downforce. It is also important to note that the coefficient of lift does not have to be scaled, meaning that once it is found in the lab it can be used in calculations of the actual airfoil.

This experiment will also have a secondary goal. The secondary goal in question being to examine how different variations of the NACA 2412 airfoil comparatively perform to one another. The variations that will be used include an unmodified normal NACA 2412 airfoil, an symmetrical NACA 0012 airfoil (Same thickness as the NACA 2412 but with no camber), and an inverted NACA 2412 airfoil where the airfoil is oriented such that the leading edge becomes the trailing edge and vise versa. It is the hope that by comparing the performances of these airfoil variants the maximum performance boost can be achieved from the NACA 2412 airfoil.

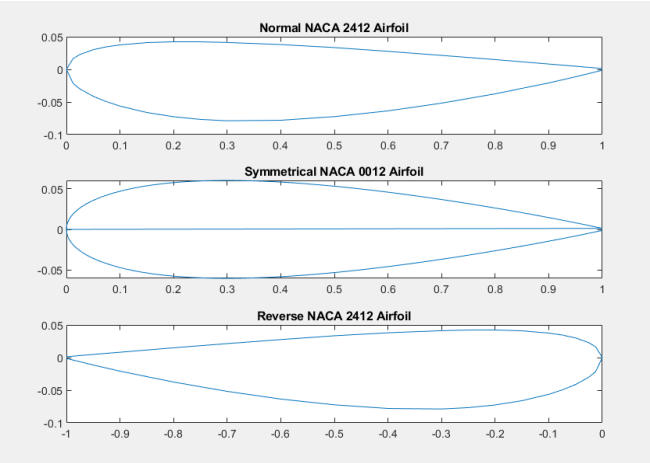

Figure 1: In the figure the profiles of the normal, symmetrical, and reverse NACA 2412 airfoil are shown. Note that as is, the airfoils air normalized by the chord

It is important to note that due to facility limitations the actual vehicle that this experiment will be attempting to improve upon will be a go kart. This is due to how the scaling parameters, Reynolds number, and wing geometry, play with the size of the UCI wind tunnel test section. If a full scale rear wing were to be examined the size of the rear wing that would have to be used in the wind tunnel would exceed the size limitations of the wind tunnel test section. As such, in order to get accurate results it was necessary to scale down the rear wing itself. In this case a go kart fits the parameters of the UCI wind tunnel test section well. The specific model of go kart that will be used is the Ninebot Gokart PRO which is able to fit an airfoil with a span of .538 meters and a chord length of .171 meters.

Interestingly the selected go kart is already equipped with a rear wing and the performance parameters of the go kart with the rear wing are provided. This includes the maximum achievable acceleration of the go kart, which is 1.02 times the acceleration due to gravity or about 10 meters per second. With this provided data this experiment can compare its acceleration data with that of the acceleration data with the original rear wing attached. This will allow for a conclusion to be made on whether the current rear wing of the go kart should be replaced with a rear wing made out of the NACA 2412 airfoil or one of its variants.

Background and Previous Work

As can be expected, a significant amount of work has been done in order to determine how various airfoils/rear wings affect the performance of cars. This allowed for this experiment to set a foundation on which to build. One such piece of work, “Effect of Steady Airflow Field On Drag and Downforce,” by S. C. Kim and S. Y. Han tests how the drag and downforce produced by a S1223 airfoil affect the performance of a car. Rather than conducting wind tunnel tests, Kim and Han made use of CFD simulations where different configurations of the S1223 airfoil were tested at different angles of attack. Similar to what is planned for this report's experiment, their experiment made use of normal, reverse, and symmetric configurations of the S1223 airfoil. The findings of their report indicate that the reverse airfoil airfoil and symmetric airfoil exhibited the best downforce to drag results.

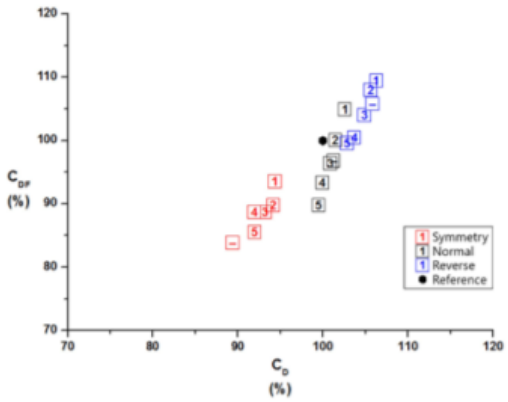

Figure 2: This figure depicts the results for S. C. Kim and S. Y. Han’s experiment. As shown with an increased coefficient of downforce there is an increased coefficient of drag. As such a careful balance needs to be made in order to maximize the advantages of downforce without increasing the total drag drastically.

This report is also able to draw data and expected data from the NACA database. This database includes the NACA 2412 airfoil and some of its variants. As such the results of this report’s experiment can be validated using known and accepted values. There will be some differences that need to be accounted for between the NACA database’s results and the results that will be obtained by this experiment. The main difference being that the data provided by the NACA database for the NACA 2412 airfoil is for a 2-D airfoil while this experiment will be using a 3-D airfoil. However, it can still be expected that the results will be similar and as such the database can be used to validate this experiment’s results.

Theoretical Presentation

Although some of the mechanics that will be used in this experiment were discussed in the introductory section of this report this section will provide a more detailed explanation for the mechanics that are responsible for the generation of downforce/lift by airfoils in general.

The first and most important mechanism that is being utilized in this report and experiment is the lift force that is generated by airfoils that are placed in a freestream flow. Lift is the result of the pressure difference generated by an airfoil. Typically the upper surface of an airfoil is designed to produce a lower pressure distribution than the lower surface. The result is a force that pushes the airfoil upwards. Typically the lifting force is designated as the force that is generated normal to the free stream flow. As such the generated distribution can be split up into normal and axial components that are in reference to the airfoil. These can then be used to calculate the lift force. The equations that are used to do so are shown below.

$$N = -\int_{TE}^{LE} \Delta P dc \qquad (Equation\ 6)$$

$$A = -\int_{TE}^{LE} \Delta P dt \qquad (Equation\ 7)$$

$$L = N\cos(\alpha) - A\sin(\alpha) \qquad (Equation\ 3)$$

The drag force can also be calculated from the pressure distribution created by an airfoil. However, unlike the lift force which is defined as being the force perpendicular to the freestream flow, the drag force is being defined as the force parallel to the freestream flow. The calculations for the drag force are very similar to those for the lift force. The normal and axial forces still need to be found. The only difference being one of trigonometry. As such the equation for the drag force can be written as follows.

$$D = N\sin(\alpha) + A\cos(\alpha) \qquad (Equation\ 8)$$

Once the lift and drag forces at different angles of attack are determined there needs to be a way to accurately scale the experimental results so that an appropriate decision can be made on what rear wing should be attached to the go kart and at what angle it should be attached. This can be achieved by finding the coefficients of lift and drag. The process for which is fairly straightforward and is defined by the equations as shown below.

$$C_L = \frac{L}{\frac{1}{2}\rho v^2 S} \qquad (Equation\ 5)$$

$$C_D = \frac{L}{\frac{1}{2}\rho v^2 S} \qquad (Equation\ 9)$$

With the coefficient of lift and drag found at varying angles of attack the results of the experiment can then be converted into expected lift and drag forces that will be incurred by the

go kart can be calculated. This can be done by rearranging the coefficient of lift and drag equations such that the drag and lift/down force are being solved for. It is important to note that the velocities and the surface area need to be set to the conditions that will be experienced by the actual go kart. In other words the velocity that the go kart will be driving at and the surface area of the rear wing that will be attached to it.

Once this is complete a simple application of Newton's second law can be utilized to calculate the new maximum acceleration that the go kart can achieve The equation that will allow this calculation is displayed below.

$$F_f = \mu N \quad (Equation\ 1)$$

$$a = \sum_{1}^{n} F_n / m \quad (Equation\ 2)$$

The basic principle that allows us to use Newton's second law is that as the rear wing produces down force the effective weight of the go karat rises. As weight is simply a normal force it can be used to calculate the maximum force that the go kart can put on the road before the tires start to slip. Using this new force combined with the fact that the actual mass of the go kart remains unchanged the new maximum achievable acceleration of the go kart can be found.

Experiment Equipment and Procedure

Equipment

1. UCI Low Speed Wind Tunnel
2. Barometer
3. Hygrometer
4. Thermometer
5. Setra Pressure Transducer
6. ATI Nano17 Force Transducer
7. NACA 2412 Normal Airfoil
8. NACA 0012 Airfoil
9. NACA 2412 Reverse Airfoil
10. Pitot Static Tube
11. Measuring Scale
12. Labview Software
13. Digital Level

Scaling Procedure

In order for the airfoil results in the wind tunnel to be used as accurate results for the go kart's rear wing appropriate scaling needs to be performed. Below are the steps on how the scaling for this experiment will be done as well as the final dimensions of the airfoils used in this experiment.

1. Find the maximum speed that the rear wing will be going on the go kart, the span and chord length of the actual rear wing, and set atmospheric conditions (STP for this lab).
2. Find the Reynolds number that is expected at the maximum speed using the chord as the length.
3. Once the Reynolds number is found for the actual go kart, set it equal to the Reynolds number that will be seen in the wind tunnel.
4. Solve for the chord length.
5. To ensure that the wing geometries remain the same set the ratio of the chord to span for the actual and model wing equal to each other and solve for the span
6. Use the resulting dimensions to build the wind tunnel test model

Table 1: Actual Rear Wing Statistics

Rear Wing Speed	10.3 m/s
Rear Wing Span	.538 m
Rear Wing Chord	.171 m

Table 2: Model Rear Wing Statistics

Model Wing Speed	35 m/s
Model Wing Span	.158 m
Model Wing Chord	.0502 m

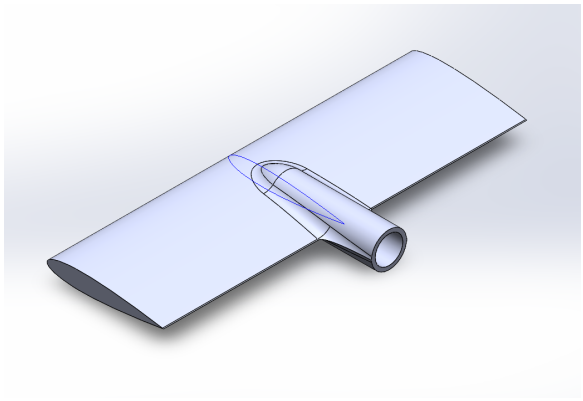

Figure 3: CAD model for the symmetrical airfoil

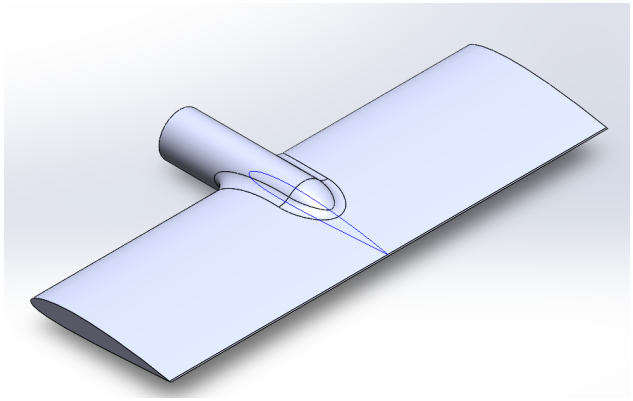

Figure 4: CAD model for the reverse airfoil

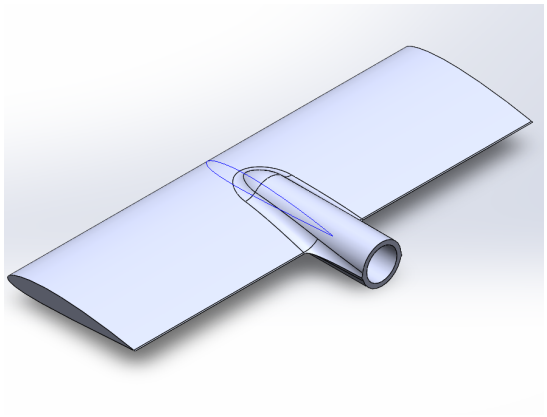

Figure 5: CAD model for the normal airfoil

Experiment Procedure

1. Using the hygrometer, barometer, and thermometer, record the pressure, temperature, and humidity of the lab facility. Use this data to calculate the local density of the air.
2. Open Labview program and make sure that the force transducer is turned on and hooked up to the computer running the Labview program.
3. Test to see if the for transducer is making valid measurements
    a. Collect a sample with nothing attached to the force transduce
    b. Set the bucking values to whatever the force transducer outputs for all degrees of freedom except for T_y
    c. Collect another sample and ensure that the outputs are all around zero. If not repeat steps a) and b)
    d. Place a known weight on the force transducer and take a sample
    e. Ensure the output from the force transducer agrees with the known value of the weight.
    f. Repeat steps a) through e) at different angles to be thorough
4. Once it is determined that the force transducer is functioning properly, mount the normal NACA 4212 airfoil to the force transducer.

5. Set all the bucking values for the force transducer to zero
6. With the wind tunnel off record the measured force in the x and z direction along with the moment about the y-axis from 6 to 22 degrees in increments of 2 degrees.
7. Place the pitot static tube into the wind tunnel test section and hook up the total pressure and static ports to the setra pressure transducer.
8. Turn the wind tunnel on
9. Using the pitot static tube get the velocity in the wind tunnel test section up to 35 m/s
10. Starting at 6 degrees take data for the force in the x and y directions as well as the moment about the y-axis
11. Repeat measurements from 6 degrees to -22 degrees, or until 2 angles after stall condition, going in increments of 2 degrees
12. Once completed repeat steps 4-11 for the symmetrical and reverse airfoils.

Experiment Results

Important Note

Originally the models used in this experiment were scaled assuming that the wind tunnel would be operating at a speed of 35 meters per second. However, during testing it was found that the wind tunnel needed to be limited to 30 meters per second due to noise considerations. The noise in question originated from small gaps between the airfoil models and mounting equipment resulting in a very loud whistling noise. However, this problem was not present at speeds of 30 m/s or lower. The result of this decrease in wind tunnel speeds means that the scaling done for the models is slightly off, affecting the final results of the experiment.

Coefficient of Lift

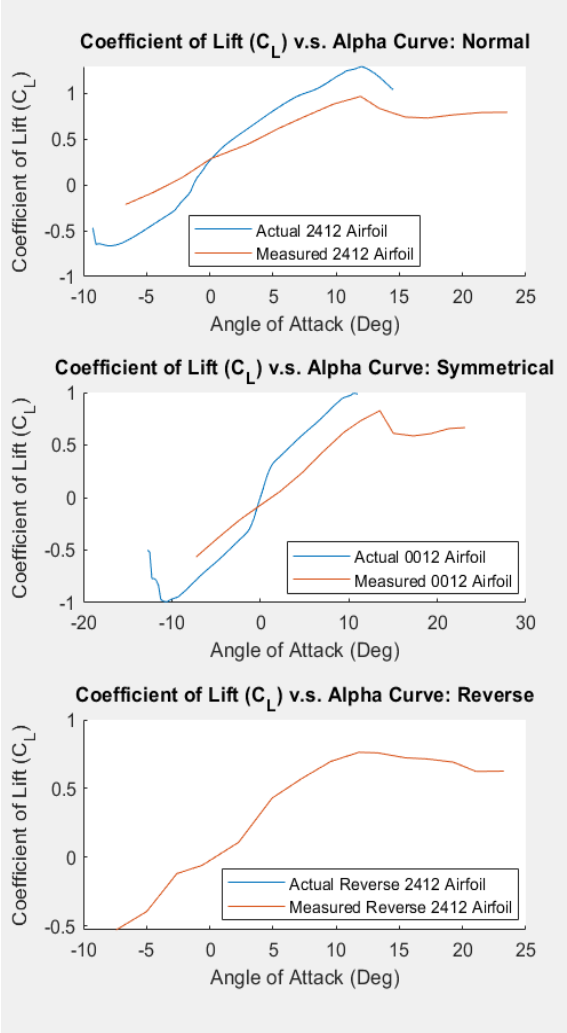

Figure 6: CL v.s. Alpha Plots at Re of 100,000

- Pictured Left is the predicted 2-D Cl v.s. Alpha curve for the normal NACA 2412 airfoil along with the actual 3-D Cl v.s. Alpha curve. As shown by the graph the actual Cl v.s. Alpha curve closely matches that of the 2-D prediction validating the collected data

- Pictured Left is the predicted 2-D Cl v.s. Alpha curve for the symmetrical NACA 0012 airfoil along with the actual 3-D Cl v.s. Alpha curve. As shown by the graph the actual Cl v.s. Alpha curve closely matches that of the 2-D prediction validating the collected data

- Pictured left is the measured 3-D Cl v.s. Alpha curve for the reverse NACA 2412 airfoil. Unfortunately, there was no available theoretical 2-D data to compare to. However, given that the results from the normal and symmetrical airfoil it can be reasoned with confidence that data displayed is vali

Coefficient of Drag

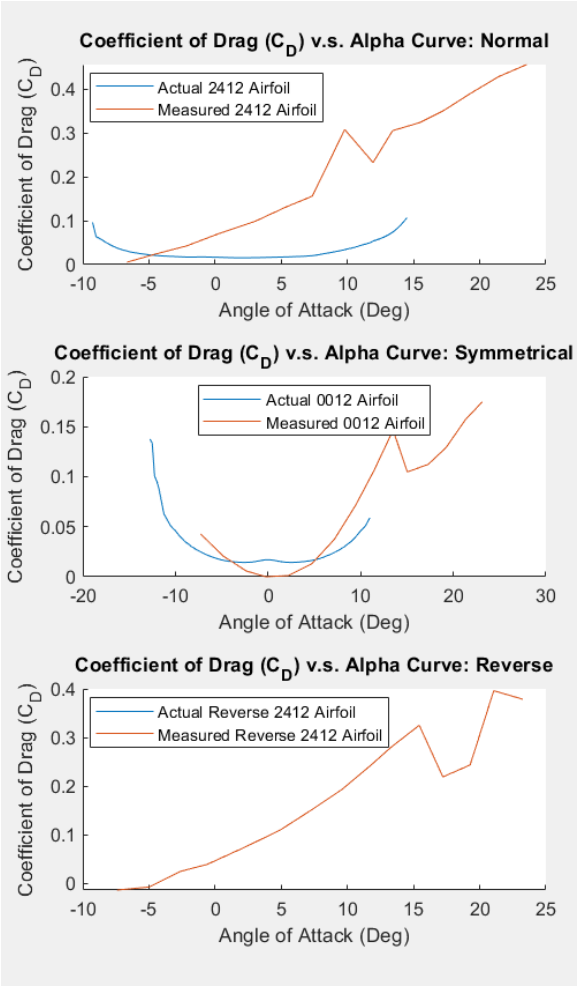

- Pictured left is predicted 2-D Cd v.s. Alpha curve plotted with the measured 3-D Cd v.s. Alpha curve for the normal NACA 2412 airfoil. As can be seen the measured Cd is higher that of the 2-D prediction

- Pictured left is predicted 2-D Cd v.s. Alpha curve plotted with the measured 3-D Cd v.s. Alpha curve for the symmetrical NACA 0012 airfoil. As shown the curve more closely resembles that of the prediction with drag increasing exponentially with angle of attack

- Pictured left is the measured 3-D Cd v.s. Alpha curve for the reverse NACA 2412 airfoil. Unfortunately there is no data to compare the results to. However, the drag is increasing exponentially as is expected.

Figure 7: CD v.s. Alpha Plots at Re of 100,000

The coefficient of drag results shown above for the three airfoil variants have been corrected using UCI's wind tunnel correction equations. As such the recorded coefficient of drag varies slightly from the corrected. The equation provided by the UCI wind tunnel laboratory for this correction is as follows.

$$C_{D_{corrected}} = C_D + .03C_L^2 \quad (Equation\ 10)$$

From these coefficients of lift and drag values the downforce and drag effects that the real airfoil would have on the go kart can be found. From there the effects that the rear wing has on the maximum achievable acceleration and turning speed can be found. The results obtained from these calculations as well as the equations used to obtain the results are shown below.

$$L = \frac{1}{2} C_L \rho V^2 S \quad (Equation\ 5)$$

$$D = \frac{1}{2} C_D \rho V^2 S \quad (Equation\ 11)$$

$$a = \frac{\mu(mg+L)-D}{m} \quad (Equation\ 12)$$

Note: It was determined that for rubber tires on asphalt a coefficient of friction of .9 would be used in the calculations.

Normal NACA 2412 Airfoil

Converting to Actual Kart			
Angle of Attack	**Downforce Actual (N)**	**Drag of Actual (N)**	**Acceleration (m/s^2)**
-22.2	3.999965844	1.130858789	8.780775186
-20.1	3.946365025	1.022012914	8.779591492
-18	3.65258204	0.843386691	8.781266853
-16	3.525754197	0.737419434	8.781426575
-14.2	3.672760908	0.6967000697	8.778047173
-12	4.96646275	1.004364732	8.761315396
-10.3	4.435017119	0.7375141364	8.765445288
-8.3	3.735751759	0.4987399285	8.773073503
-6.1	2.65300228	0.2587257834	8.787418432
-4.3	1.4083873	0.0863547977	8.805929809
-2.3	0.337862791	0.006890023807	8.823195576
0.4	-0.5264313377	0.001033020747	8.838273852
2.3	-1.290594698	0.04278639938	8.852521907
4.3	-2.340660027	0.1522665581	8.873118371
6.3	-3.401744469	0.3142051113	8.894933108

Symmetrical NACA 0012 Airfoil

Converting to Actual Kart			
Angle of Attack	**Downforce Actual (N)**	**Drag of Actual (N)**	**Acceleration (m/s^2)**

-22	4.755401002	2.852147792	8.856885022
-20.2	4.736467177	2.687401279	8.859769906
-18.2	4.587228612	2.449153471	8.861799849
-16.3	4.377394769	2.201130425	8.862955564
-14	4.43858333	2.042391807	8.867131508
-12.1	5.003192475	1.959539476	8.878674487
-10.2	5.793369756	1.565413321	8.900262099
-8.4	5.291001025	1.988951484	8.883159169
-6.4	4.409363524	1.034423685	8.886304756
-4.3	3.651759577	0.8531012505	8.876528953
-2.1	2.675948601	0.6313878159	8.863706366
0.1	1.710122054	0.4255156699	8.850749886
2	0.4873862757	0.2562846569	8.832561777
4.2	-0.4840888971	0.14890891	8.817582248
6.3	-1.292188285	0.04074004887	8.805490049

Reverse NACA 2412 Airfoil

Converting to Actual Kart			
Angle of Attack	**Downforce Actual (N)**	**Drag of Actual (N)**	**Acceleration (m/s^2)**
-22.2	3.76233327	2.346052088	8.849313435
-20	3.748468486	2.451093428	8.847018129
-18.1	4.154429009	1.549468528	8.871764015
-16	4.29486544	1.407575628	8.87700397
-14.2	4.348438242	2.048247838	8.86543255
-12	4.562769668	1.785312881	8.874335543
-10.5	4.586871649	1.568465733	8.878994507
-8.4	4.189221144	1.247475948	8.878273888
-6.3	3.436722247	0.964727108	8.870568807
-4.2	2.582359633	0.6926333187	8.860865046
-2.1	0.6483422217	0.4513212904	8.831581772
0.5	-0.3589342899	0.2342821089	8.818114786
2.4	-0.7211853781	0.1502450151	8.81338844
4.3	-2.37084084	-0.01784684861	8.787673635
6.5	-3.185579302	-0.03281287195	8.773644365

Analysis of Results

By taking the raw coefficient of lift and drag data acquired by the experiment the effect that the downforce induced by the go kart rear wing has on performance was calculated. Given that the coefficient of lift changes with angle of attack there are two decisions that need to be made. The first being which NACA 2412 variant should be used as the rear wing. The second being at what angle of attack should this NACA 2412 variant be set to.

By looking at the results above it can be seen that the maximum achievable acceleration for the go kart with a NACA 2412 variant wing installed occurs when the normal airfoil is at an angle of attack of -12 degrees, the symmetrical airfoil is at an angle of attack of -10.2 degrees, and the reverse airfoil is at an angle of attack of -10.5 degrees. At these angles of attack the maximum achievable acceleration by the airfoil variants are 8.9, 8.897, and 8.879 meters per second squared respectively. It is important to note that all of these values are lower than the maximum acceleration allowed by the original airfoil installed on the go kart. As such, for this go kart and the speed that it travels it can be determined that none of the NACA 2412 variants are viable options as a rear wing.

Conclusion

In this report the effects of NACA 2412 derived rear wing variants were studied to determine their effects on the maximum acceleration that could be achieved by a go kart. The go kart in particular that was used as a model was the Ninebot Gokart PRO. This go kart is already equipped with a rear wing affording the go kart a maximum acceleration of 10 meters per second squared. As such this go kart in particular provided a good base from which to compare the results that were found using the NACA 2412 variants.

In order to find the effects that the NACA 2412 variants had on the selected go kart, scaled models of the rear wings were created and placed into the UCI laboratory facility's wind tunnel. By running the wind tunnel at a speed determined by the scaling process for the rear wing models and through the use of a force transducer the lift and drag coefficients at varying angles of attack were found. This was done for each NACA 2412 airfoil variant: normal, symmetrical, and reversed.

Unfortunately due to small compatibility issues between the airfoils and the force transducer mount the speed at which the wind tunnel tests occurred were about 5 meters per second slower than what the experiment design called for. As a result the scaling of the airfoils became off. In order to calculate the real world effects that the NACA 2412 variants would have on the go-kart it is important to keep the scaling constant. As such, this change of speed resulted in an altering of the final results of the experiment. Fortunately, since the difference in speed was relatively small it can be assumed, with some confidence that the results are similar to what would be expected.

Once all of the calculations and transformations from scale to real model rear wings were conducted it was found that out of the NACA 2412 airfoil variants the normal airfoil at an angle of attack of -12 degrees yields a maximum acceleration of 8.9 meters per second squared. This is about 1.1 meters per second squared slower acceleration than what the go kart with the original rear wing could achieve. As such it can be concluded that none of the rear wing options presented in this report can be recommended as rear wings for the Ninebot Gokart PRO go kart. Instead, the original rear wing should be kept on the go kart in order to ensure the maximum acceleration.

Acknowledgements

This report thanks the NACA database for providing values off of which this report's data could be compared against. This report thanks Kristian Aguilar, Zhuohuan Li, Braeden Ciukowski, Zandro Mara, Chaz Fazio, Ethan Leong, and Wessam Elmasri for helping to conduct this experiment. In addition this report thanks Deb Dipan for assisting in the smooth operation of the wind tunnel as well as providing additional assistance and knowledge to this experiment. Finally this report thanks Dr. Jacqueline L. Huynh for approving the conduction of this experiment, providing theoretical knowledge, and providing the facility in which this experiment was conducted.

References

Kim, S. C., and S. Y. Han. "Effect of Steady Airflow Field on Drag and Downforce." International Journal of Automotive Technology, The Korean Society of Automotive Engineers, 9 Apr. 2016, https://link.springer.com/article/10.1007/s12239-016-0020-2.

LaRue, J, et all "MAE 108 Aerospace Laboratory Manual." University of California Irvine, 2017, https://canvas.eee.uci.edu/courses/40137/files/15710885?wrap=1

"Gokart Pro-Specs." Segway, https://www.segway.com/ninebot-gokart-pro/gokart-pro-specs/#specs-gkp.

Appendix

Appendix A: Raw Collected Data

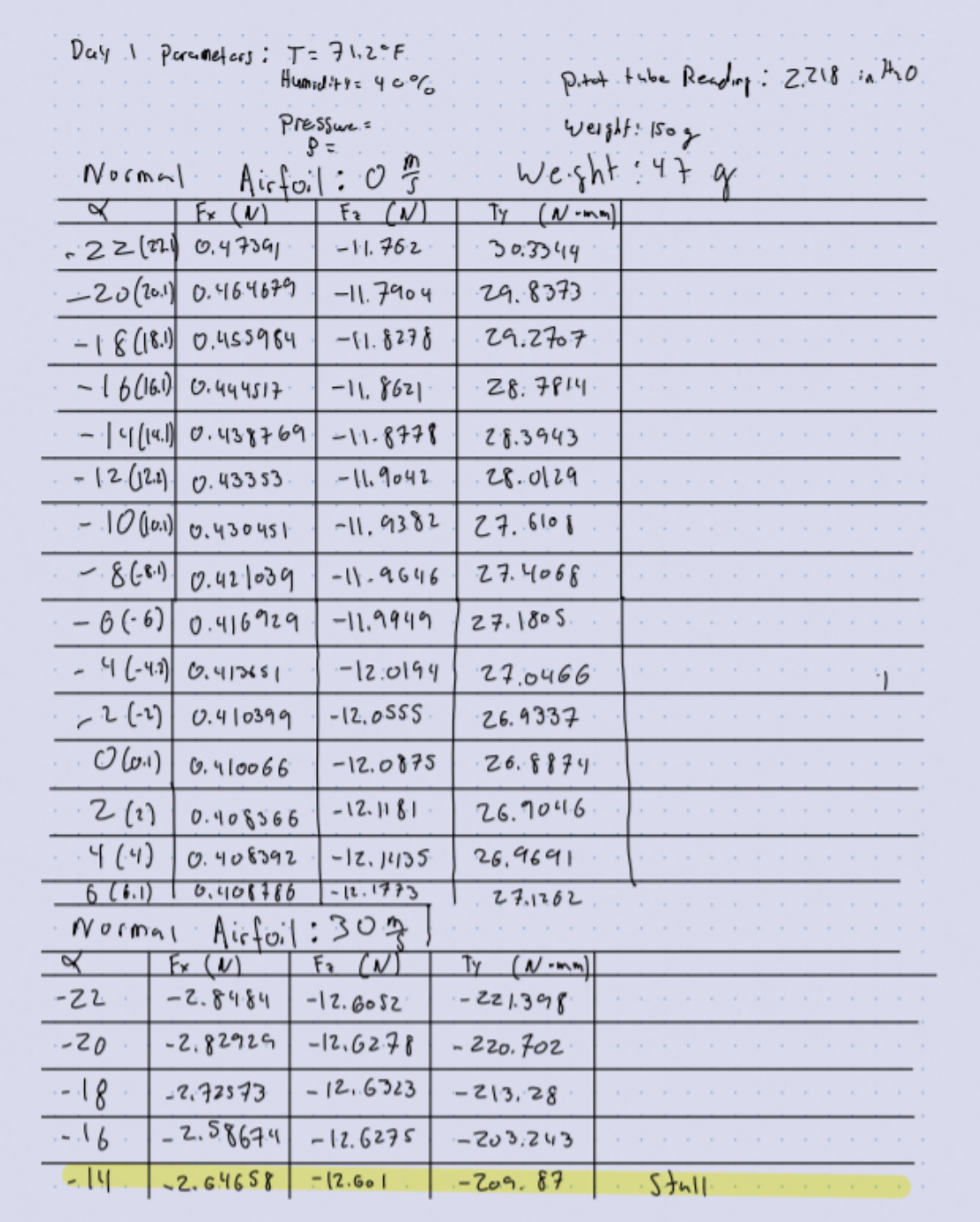

Day 1 Parameters: T = 71.2°F
Humidity = 40%
Pressure = ρ =
Pitot tube Reading: 2.218 in H_2O
Weight: 150 g

Normal Airfoil: 0 m/s — Weight: 47 g

α	Fx (N)	Fz (N)	Ty (N-mm)
-22 (22.1)	0.473991	-11.762	30.3344
-20 (20.1)	0.464879	-11.7904	29.8373
-18 (18.1)	0.455984	-11.8278	29.2707
-16 (16.1)	0.444517	-11.8621	28.7814
-14 (14.1)	0.438769	-11.8778	28.3943
-12 (12.1)	0.43353	-11.9042	28.0129
-10 (10.1)	0.430451	-11.9382	27.6108
-8 (-8.1)	0.421039	-11.9646	27.4068
-6 (-6)	0.416929	-11.9949	27.1805
-4 (-4.1)	0.412651	-12.0194	27.0466
-2 (-2)	0.410399	-12.0555	26.9337
0 (0.1)	0.410066	-12.0875	26.8874
2 (2)	0.408366	-12.1181	26.7046
4 (4)	0.408392	-12.1435	26.9691
6 (6.1)	0.408786	-12.1773	27.1262

Normal Airfoil: 30 m/s

α	Fx (N)	Fz (N)	Ty (N-mm)	
-22	-2.8484	-12.6052	-221.398	
-20	-2.82929	-12.6278	-220.702	
-18	-2.72573	-12.6323	-213.28	
-16	-2.58674	-12.6275	-203.243	
-14	-2.64658	-12.601	-209.87	Stall

-12	-3.07221	-12.8891	-246.301
-10	-3.70249	-12.3228	-313.284
-8	-3.26505	-12.3669	-277.334
-6	-2.70491	-12.4039	-230.766
-4	-2.1692	-12.4359	-186.857
-2	-1.48681	-12.4304	-130.692
0	-0.812915	-12.3998	-73.5621
2	0.0522263	-12.3155	-0.699226
4	0.748824	-12.2245	59.2763
6	1.345	-12.1032	110.51

Inverted Airfoil: 0 m/s Weight: 47g

α	Fx (N)	Fz (N)	Ty (N-mm)
-22(22.1)	0.602341	-11.8657	30.1739
-20(20)	0.598039	-11.8831	29.6586
-18(18.1)	0.588023	-11.9123	29.21
-16(16.1)	0.584303	-11.9333	28.9443
-14(14.1)	0.565862	-11.9578	28.4585
-12(12.1)	0.55731	-11.9909	27.9861
-10(10.2)	0.55494	-12.018	27.6574
-8(8.3)	0.550414	-12.0455	27.3967
-6(6.3)	0.543129	-12.0743	27.2067
-4(4.1)	0.539599	-12.1075	27.0433
-2(2.4)	0.530582	-12.1294	26.9614
0(0.3)	0.536522	-12.1622	26.8992
2(2)	0.539642	-12.1932	26.8971

4 (4.3)	0.5309934	-12.2759	26.9355
6 (6)	0.544044	-12.2539	27.0318

Inverted Airfoil : 30 m/s

α	Fx (N)	Fz (N)	Ty (N-mm)	
-22 (22.2)	-2.51709	-12.4015	-223.024	
-20 (20)	-2.51487	-12.621	-223.50	
-18 (18.4)	-2.5745	-12.0123	-228.424	
-16 (16)	-2.63978	-12.6541	-233.471	
-14 (14.2)	-2.80215	-12.6138	-247.8	Stall
-12 (12)	-2.89362	-12.5603	-260.464	
-10 (10.3)	-2.86861	-12.5222	-263.165	
-8 (8.4)	-2.53807	-12.4898	-237.879	
-6 (6.3)	-1.97077	-12.4656	-187.759	
-4 (4.2)	-1.33508	-12.4344	-131.222	
-2 (2.1)	0.0562679	-12.3272	-16.8612	
0 (0.5)	0.794197	-12.2788	49.2464	
2 (2.4)	1.65558	-12.1698	122.931	
4 (4.3)	2.22664	-12.0863	175.04	
6 (6.5)	2.80806	-11.9732	227.783	

Symmetric Airfoil : 0 m/s weight : 57 g

α	Fx (N)	Fz (N)	Ty (N-mm)
-22 (-22)	0.520356	-11.8435	19.7158
-20 (20.1)	0.509703	-11.8686	19.1455
-18 (18.1)	0.499246	-11.9125	18.4964
-16 (16)	0.488571	-11.9451	17.9734
-14 (14.1)	0.477835	-11.9646	17.522
-12 (12.3)	[illegible]	[illegible]	[illegible]

−10(10)	0.46547	−12.0218	16.7775
−8(8.3)	0.462986	−12.0548	16.441
−6(6.3)	0.460735	−12.0788	16.2203
−4(4)	0.459983	−12.1171	16.0378
−2(2)	0.457076	−12.1482	15.9305
0(0.3)	0.45257	−12.1795	15.927
2(2.1)	0.456127	−12.2183	15.9214
4(4.1)	0.457989	−12.2481	16.0057
6(6.3)	0.459112	−12.2865	16.1914

Symmetric Airfoil : 30 m/s

α	Fx (N)	Fz (N)	Ty (N·mm)	
−22(22)	−2.27863	−12.3381	−193.476	
−20(20.2)	−2.2417	−12.549	−191.225	
−18(18.1)	−2.03537	−12.5515	−176.274	
−16(16)	−1.95932	−12.5414	−171.455	
−14(14)	−2.09211	−12.4945	−183.904	St411
−12(12)	−3.11765	−12.1615	−283.76	
−10(10)	−2.71363	−12.2312	−249.175	
−8(8.4)	−2.19912	−12.7822	−206.596	
−6(6.4)	−1.41975	−12.3038	−144.094	
−4(4.3)	−0.535187	−12.2906	−72.6112	
−2(2.1)	0.219522	−12.2516	−9.15056	
0(0.1)	0.828282	−12.2263	44.0748	
2(2)	1.37967	−12.1699	92.8852	
4(4.2)	2.14857	−12.0411	158.308	
6(6.3)	2.95207	−11.8348	224.577	

Appendix B: Digitized Data and Calculation Results

Global Variables (Day 1)			
Temperature =	71.4		F
Humidity =	39%		%
Pressure =	29.9		inHg
Density =	1.19098		kg/m^3
q*S	4.290668614		

Tunnel Off	Weight =	57	g	
Symmetric Airfoil		**Fx**	**Fz**	**Ty**
Ideal Angle	Actual Angle	Normal (N)	Axial (N)	Pitch (N.mm)
-22	-22	0.520356	-11.8435	19.7158
-20	-20.1	0.509703	-11.8686	19.1455
-18	-18.1	0.499246	-11.9125	18.4964
-16	-16.1	0.488571	-11.9451	17.9734
-14	-14.1	0.477835	-11.9646	17.522
-12	-12.3	0.471256	-11.9901	17.1594
-10	-10	0.46547	-12.0218	16.7775
-8	-8.3	0.462986	-12.0548	16.441
-6	-6.3	0.460735	-12.0788	16.2203
-4	-4	0.459983	-12.1171	16.0378
-2	-2	0.457076	-12.1482	15.9305
0	0.3	0.45257	-12.1795	15.927
2	-2.1	0.456127	-12.2183	15.9214
4	-4.1	0.457989	-12.2481	16.0057
6	-6.3	0.459112	-12.2865	16.1914

Tunnel Speed = 30 m/s

Symmetric Airfoil			Fx	Fz	Ty	Calibrated					Calibrated					
Ideal Angle	Actual Angle	Radians	Normal (N)	Axial (N)	Pitch (N.mm)	Normal (N)	Axial (N)	Normal cos (N)	Axial sin (N)	Lift (N)	Normal sin (N)	Axial cos (N)	Drag (N)	Corrected Alpha	CL	CD Corrected
-22	-22	-0.383972435	-2.27863	-12.5381	-193.476	-2.798986	-0.6946	-2.595174628	0.2602017398	-2.855376368	-1.04851861	0.2412548521	-0.8072637584	23.13150112	0.665588897	-0.1748831129
-20	-20.2	-0.352556508	-2.2417	-12.549	-191.225	-2.751403	-0.6804	-2.582172518	0.2349408946	-2.817113413	-0.9500545006	0.2204903903	-0.7295641103	21.31633865	0.6566697932	-0.1571251076
-18	-18.2	-0.317649923	-2.03537	-12.5515	-176.274	-2.534616	-0.639	-2.407814361	0.1995820129	-2.607396374	-0.7916490818	0.1895973343	-0.6020517475	19.23323399	0.6077847026	-0.1292563353
-16	-16.3	-0.284488666	-1.95932	-12.5414	-171.455	-2.447891	-0.5963	-2.349498736	0.1673615585	-2.516860295	-0.6870415108	0.1606345095	-0.5264070012	17.29735723	0.5866807213	-0.1123797666
-14	-14	-0.244346095	-2.09211	-12.4945	-183.904	-2.569945	-0.5299	-2.49360665	0.1281944125	-2.621801063	-0.621725966	0.1243864906	-0.4973394754	15.03894215	0.6111424389	-0.1047250952
-12	-12.1	-0.211184835	-3.11765	-12.1625	-283.76	-3.588906	-0.1724	-3.509172125	0.0361382402	-3.545310365	-0.7523013181	0.03533536552	-0.7169659526	13.50490154	0.8264126726	-0.1466361935
-10	-10.2	-0.178023588	-2.71363	-12.2312	-249.1755	-3.1791	-0.2094	-3.128856257	0.0370815446	-3.165937802	-0.5629700979	0.03649549335	-0.5264746046	11.45456743	0.7379808396	-0.1063828815
-8	-8.4	-0.146607657	-2.19912	-12.2822	-206.596	-2.662106	-0.2274	-2.633547813	0.0332192807	-2.666767094	-0.3888885068	0.03286291531	-0.3560255915	9.456760853	0.6216240312	-0.07139715529
-6	-6.4	-0.111701077	-1.41975	-12.3038	-144.094	-1.880485	-0.225	-1.868765665	0.0250805097	-1.893846175	-0.209615655	0.02492420598	-0.1846911449	7.150475174	0.4414559849	-0.03720511821
-4	-4.3	-0.075049157	-0.535187	-12.2906	-72.6112	-0.99517	-0.1735	-0.9923687293	0.0130088091	-1.005377538	-0.07461657958	0.01297219104	-0.0616443885	4.698401356	0.2343537386	-0.01272167109
-2	-2.1	-0.036651914	0.219522	-12.2516	-9.15056	-0.237554	-0.1034	-0.2373944573	0.0037889594	-0.241834167	-0.00870485978	0.00378614791	-0.0049184447	2.195573848	0.05621991066	-0.00105167027
0	0.1	0.001745329	0.828282	-12.2263	44.0748	0.375712	-0.0468	0.3757114278	-0.0000816813	0.3757931091	-0.000655740811	-0.00008168124312	-0.0007374220	-0.2489156843	-0.08759746133	0.000058306204
2	2	0.034906585	1.37967	-12.1699	92.8852	0.923543	0.0484	0.9229804026	0.0016891356	0.9212912669	-0.03223118588	0.001688106665	-0.0305430792	-2.365080455	-0.2147532091	-0.00573603066
4	4.2	0.073303828	2.14857	-12.0411	158.308	1.690581	0.207	1.686040906	0.0151603068	1.670880599	-0.1238151045	0.01511959346	-0.1086955111	-4.862120517	-0.3894826572	-0.02078604676
6	6.3	0.109955742	2.95207	-11.8348	224.577	2.492958	0.4517	2.477902916	0.0495669883	2.428335927	-0.2735630287	0.04926765107	-0.2242953776	-7.26227764	-0.5660456707	-0.04267107377

Tunnel Off	Weight =	47	g	Ty
Normal Airfoil		Fx	Fz	Pitch (N.mm)
Ideal Angle	Actual Angle	Normal (N)	Axial (N)	30.3344
-22	-22.1	0.473931	-11.762	29.8373
-20	-20.1	0.464679	-11.7904	29.2707
-18	-18.1	0.455984	-11.8278	28.7814
-16	-16.1	0.444517	-11.8621	28.3943
-14	-14.1	0.438769	-11.8778	28.0129
-12	-12.2	0.43353	-11.9042	27.6108
-10	-10.1	0.430451	-11.9382	27.4068
-8	-8.1	0.421039	-11.9646	27.1805
-6	-6	0.416929	-11.9949	27.0466
-4	-4.2	0.413651	-12.0194	26.9337
-2	-2	0.410399	-12.0555	26.8874
0	0.1	0.410066	-12.0875	26.9046
2	2	0.408366	-12.1181	26.9691
4	4	0.408392	-12.1435	27.1262
6	6.1	0.408786	-12.1773	

	Actual Speed																
Tunnel Speed =	30	m/s															
Normal Airfoil			Fx	Fz	Ty	Calibrated						Calibrated					
Ideal Angle	Actual Angle	Radians	Normal (N)	Axial (N)	Pitch (N.mm)	Normal (N)	Axial (N)	Normal cos (N)	Axial sin (N)	Lift (N)		Normal sin (N)	Axial cos (N)	Drag (N)	Corrected Alpha	CL	CD Corrected
-22	-22.2	-0.387463095	-2.8484	-12.6052	-221.398	-3.322331	-0.8432	-3.076048546	0.3185953514	-3.394643897		-1.255312159	-0.7806940771	-2.036006236	23.54519688	0.7912922838	-0.4558092239
-20	-20.1	-0.350811175	-2.82929	-12.6278	-220.702	-3.293969	-0.8374	-3.093347354	0.2877806282	-3.381127983		-1.132004381	-0.7863975267	-1.918401907	21.43984093	0.7881417209	-0.4285449106
-18	-18	-0.314159265	-2.72573	-12.6323	-213.28	-3.181714	-0.8045	-3.025989833	0.248604172	-3.274594005		-0.9832036972	-0.7651249674	-1.748328665	19.29762466	0.7633086258	-0.3900566175
-16	-16	-0.279252680	-2.58674	-12.6275	-203.243	-3.031257	-0.7654	-2.913831245	0.2109728321	-3.124804077		-0.8355276643	-0.7357497021	-1.571277366	17.23826735	0.7283925587	-0.3503484488
-14	-14.2	-0.247836753	-2.64658	-12.601	-209.87	-3.085349	-0.7232	-2.991077241	0.1774063015	-3.168483542		-0.7568588977	-0.701102877	-1.457961775	15.45557623	0.7385742523	-0.3234864718
-12	-12	-0.209439510	-3.07221	-12.5891	-246.301	-3.50574	-0.6849	-3.42913117	0.142398717	-3.571529887		-0.728884331	-0.6699332917	-1.398817623	13.41529156	0.8325244491	-0.3052718052
-10	-10.3	-0.179768913	-3.70299	-12.3228	-313.284	-4.133441	-0.3846	-4.066830755	0.06876733195	-4.135598087		-0.7390684069	-0.3784021856	-1.117470592	11.93881509	0.9640088781	-0.2326032621
-8	-8.3	-0.144862327	-3.26505	-12.8617	-277.339	-3.686089	-0.8971	-3.647480126	0.1295019479	-3.776982074		-0.5321098046	-0.8877035854	-1.41981339	9.796706183	0.8804154019	-0.3077048938
-6	-6.1	-0.106465084	-2.70491	-12.4039	-230.766	-3.121839	-0.409	-3.104162973	0.043462005182	-3.147624978		-0.3317393222	-0.4066842192	-0.7384235413	7.347310597	0.7337121162	-0.1559766955
-4	-4.3	-0.075049157	-2.1692	-12.4359	-186.857	-2.582851	-0.4165	-2.575580619	0.031228639726	-2.606809259		-0.1936588796	-0.4153276081	-0.6089864877	5.333001338	0.6076478459	-0.1308778151
-2	-2.3	-0.040142572	-1.48631	-12.4304	-130.692	-1.896709	-0.3749	-1.895181002	0.015045409026	-1.910226411		-0.07611833208	-0.3745979787	-0.4507163108	3.056966177	0.4452742217	-0.09911400314
0	0.4	0.006981317(	-0.812915	-12.3998	-73.5621	-1.222981	-0.3123	-1.222951197	-0.002180247539	-1.220770949		0.0085379487	-0.3122923895	-0.3037544408	0.0837553878	0.2845619928	-0.06837596512
2	2.3	0.040142572(	0.0522363	-12.3155	-0.699226	-0.3561297	-0.1974	-0.355842800	-0.007922015858	-0.347920784		0.01429212324	-0.1972409736	-0.1829488504	-2.162129293	0.08110041593	-0.04244810134
4	4.3	0.075049157(	0.748844	-12.2245	59.2763	0.340452	-0.081	0.339493673	-0.006073276837	0.34556695		-0.02552665751	-0.08077199582	-0.1062986533	-4.436937952	-0.08055173659	-0.02458358344
6	6.3	0.109955742(	1.345	-12.1032	110.51	0.936214	0.0741	0.930560162	0.008131312454	0.9224288495		-0.1027347983	0.0736525068	-0.0290822915(	-6.665531246	-0.2150183798	-0.00539210182

Tunnel Off	Weight =	47	g	Ty
Inverted Airfoil		Fx	Fz	Pitch (N.mm)
Ideal Angle	Actual Angle	Normal (N)	Axial (N)	
-22	-22.1	0.602341	-11.8657	30.1739
-20	-20.3	0.598039	-11.8831	29.6586
-18	-18.3	0.588023	-11.9123	29.21
-16	-16.5	0.584303	-11.9333	28.9443
-14	-14.1	0.565862	-11.9578	28.4585
-12	-12.4	0.55731	-11.9909	27.9861
-10	-10.2	0.55494	-12.018	27.6574
-8	-8.3	0.550414	-12.0455	27.3967
-6	-6.3	0.54329	-12.0743	27.2067
-4	-4.1	0.539599	-12.1075	27.0433
-2	-2.4	0.530582	-12.1294	26.914
0	0.3	0.536522	-12.1622	26.8992
2	2	0.536942	-12.1932	26.8971
4	4.3	0.539934	-12.2259	26.9355
6	6	0.544049	-12.2539	27.0318

	Actual Speed															
Tunnel Speed =	30	m/s														
Reverse Airfoil			Fx	Fz	Ty	Calibrated					Calibrated					
Ideal Angle	Actual Angle	Radians	Normal (N)	Axial (N)	Pitch (N.mm)	Normal (N)	Axial (N)	Normal cos (N)	Axial sin (N)	Lift (N)	Normal sin (N)	Axial cos (N)	Drag (N)	Correced Alpha	CL	CD Corrected
-22	-22.2	0.387463093	-2.51709	-12.4015	-223.024	-3.119431	-0.5358	-2.888189404	-0.2024470936	-2.685742311	-1.178648263	-0.4960814593	-1.674729723	23.26428017	0.6260471587	-0.3786218374
-20	-20	0.349065850	-2.51487	-12.6121	-223.5	-3.112909	-0.729	-2.925177616	-0.2493326845	-2.675844932	-1.064677582	-0.6850359206	-1.749713503	21.06035813	0.6237400774	-0.3961870749
-18	-18.1	0.315904594	-2.5745	-12.0423	-228.424	-3.162523	-0.13	-3.006027863	-0.0403879358	-2.965639927	-0.9825213543	-0.1235670451	-1.106088399	19.27519531	0.6912913583	-0.2434929515
-16	-16	0.279252680	-2.63978	-12.0541	-233.471	-3.224083	-0.1208	-3.099187492	-0.0332969925	-3.0658905	-0.8886777131	-0.1161204129	-1.004798126	17.21492164	0.7146597902	-0.2188965189
-14	-14.2	0.247836753	-2.8021	-12.6138	-247.8	-3.367962	-0.656	-3.2650551	-0.1609216451	-3.104133454	-0.826185954	-0.6359561495	-1.462142103	15.43007619	0.7235742318	-0.3251188751
-12	-12	0.209439510	-2.89362	-12.5603	-260.464	-3.45093	-0.5694	-3.3755189	-0.1183849168	-3.257133983	-0.7174886912	-0.5569572439	-1.274445935	13.29070577	0.7592386907	-0.2797803429
-10	-10.5	0.183259571	-2.86861	-12.5222	-263.165	-3.42355	-0.5042	-3.366222339	-0.0918831519	-3.274339187	-0.6238924333	-0.4957571244	-1.119649558	11.79752369	0.7632492277	-0.2435140914
-8	-8.4	0.146607657	-2.53807	-12.4896	-237.879	-3.088484	-0.4441	-3.055351772	-0.0648754729	-2.990476299	-0.4511750964	-0.4393358431	-0.8905109395	9.585037228	0.6970807224	-0.1930006616
-6	-6.3	0.109955742	-1.97077	-12.4896	-187.759	-2.51406	-0.4153	-2.49887748	-0.0455726594	-2.45330482	-0.2758786421	-0.4127919848	-0.6886706269	7.272172073	0.5718659255	-0.1507183646
-4	-4.2	0.073303828	-1.33508	-12.4656	-131.222	-1.874679	-0.3581	-1.869644507	-0.0262265983	-1.843417908	-0.1372981102	-0.3571383143	-0.4944364244	4.930491945	0.4297011442	-0.1097139536
-2	-2.1	0.036651914	0.0562679	-12.4344	-16.8612	-0.4743141	-0.305	-0.4739955477	-0.0111763311	-0.4628192165	-0.01738062772	-0.3047951601	-0.3221757878	2.283401554	0.1078832673	-0.07475008726
0	0.5	-0.008726646	0.794197	-12.3272	49.2464	0.257675	-0.165	0.2576651885	0.0014398783	0.2562253102	-0.002248610035	-0.1649937173	-0.1672423273	-0.6015345052	-0.05972617953	-0.03887720899
2	2.4	-0.041887902	1.0558	-12.2788	122.931	0.518858	-0.0856	0.5184028734	0.0035845559	0.5148183174	-0.02172751794	-0.08552491426	-0.1072524322	-2.604007259	-0.1200042698	-0.0245685362
4	4.3	-0.075049157	2.22664	-12.0863	175.04	1.686706	0.1396	1.681958148	-0.0104670302	1.692425178	-0.1264670684	0.1392070446	0.01273997623	-4.970657996	-0.3945047035	0.007638710262
6	6.5	-0.113446401	2.800806	-11.9732	227.783	2.256757	0.2807	2.24225024	-0.0317761421	2.274026382	-0.2554721451	0.2788956199	0.0234234748	-7.401129336	-0.5300760798	0.013889436955

Normal NACA 2412 Airfoil

Converting to Actual Kart			
Angle of Attack	**Downforce Actual (N)**	**Drag of Actual (N)**	**Acceleration (m/s^2)**
-22.2	3.999965844	1.130858789	8.780775186
-20.1	3.946365025	1.022012914	8.779591492
-18	3.65258204	0.843386691	8.781266853
-16	3.525754197	0.737419434	8.781426575
-14.2	3.672760908	0.6967000697	8.778047173
-12	4.96646275	1.004364732	8.761315396
-10.3	4.435017119	0.7375141364	8.765445288
-8.3	3.735751759	0.4987399285	8.773073503
-6.1	2.65300228	0.2587257834	8.787418432
-4.3	1.4083873	0.0863547977	8.805929809
-2.3	0.337862791	0.006890023807	8.823195576
0.4	-0.5264313377	0.001033020747	8.838273852
2.3	-1.290594698	0.04278639938	8.852521907
4.3	-2.340660027	0.1522665581	8.873118371
6.3	-3.401744469	0.3142051113	8.894933108

Symmetrical NACA 0012 Airfoil

Converting to Actual Kart			
Angle of Attack	**Downforce Actual (N)**	**Drag of Actual (N)**	**Acceleration (m/s^2)**
-22	4.755401002	2.852147792	8.856885022
-20.2	4.736467177	2.687401279	8.859769906

-18.2	4.587228612	2.449153471	8.861799849
-16.3	4.377394769	2.201130425	8.862955564
-14	4.43858333	2.042391807	8.867131508
-12.1	5.003192475	1.959539476	8.878674487
-10.2	5.793369756	1.565413321	8.900262099
-8.4	5.291001025	1.988951484	8.883159169
-6.4	4.409363524	1.034423685	8.886304756
-4.3	3.651759577	0.8531012505	8.876528953
-2.1	2.675948601	0.6313878159	8.863706366
0.1	1.710122054	0.4255156699	8.850749886
2	0.4873862757	0.2562846569	8.832561777
4.2	-0.4840888971	0.14890891	8.817582248
6.3	-1.292188285	0.04074004887	8.805490049

Reverse NACA 2412 Airfoil

Converting to Actual Kart			
Angle of Attack	**Downforce Actual (N)**	**Drag of Actual (N)**	**Acceleration (m/s^2)**
-22.2	3.76233327	2.346052088	8.849313435
-20	3.748468486	2.451093428	8.847018129
-18.1	4.154429009	1.549468528	8.871764015
-16	4.29486544	1.407575628	8.87700397
-14.2	4.348438242	2.048247838	8.86543255
-12	4.562769668	1.785312881	8.874335543
-10.5	4.586871649	1.568465733	8.878994507
-8.4	4.189221144	1.247475948	8.878273888
-6.3	3.436722247	0.964727108	8.870568807
-4.2	2.582359633	0.6926333187	8.860865046
-2.1	0.6483422217	0.4513212904	8.831581772
0.5	-0.3589342899	0.2342821089	8.818114786
2.4	-0.7211853781	0.1502450151	8.81338844
4.3	-2.37084084	-0.01784684861	8.787673635
6.5	-3.185579302	-0.03281287195	8.773644365

Appendix C: Cad Model Mount Dimensions